Crystal Engineering for Achievement of Functional Materials Through Facile Intercalation of Lamella Mineral Kaolinite

Xin Sun[1], Yuxuan Zhang[1], Hao Yang[2,*] and Xiao-Ming Ren[3]

[1]*Suzhou North America High School, Suzhou 215000, Jiangsu, PR China*

[2]*Institute of Functional Nano&Soft Materials (FUNSOM), Jiangsu Key Laboratory for Carbon-Based Functional Materials & Devices, Soochow University, Suzhou 215123, Jiangsu, PR China*

[3]*State Key Laboratory of Materials-Oriented Chemical Engineering and College of Chemistry and Molecular Engineering, Nanjing Tech University, Nanjing 210009, Jiangsu, PR China*

Abstract: Kaolinite, a layered clay mineral, has attracted widely attention due to its versatile advantages including low cost, environmentally friendly processing and easy modification. By comparison of the wide studies of the intercalation processes of kaolinite via the replacement of diverse intercalated agents, the multiple functional properties of intercalated kaolinites are ignored as well as such kind of study is very limited. In this review, we have summarized a series of intercalated compounds of kaolinites with organic molecules or organic salts by means of a simple intercalation strategy. Additionally, their multiple functional properties (such as dielectricity, ferroelectricity and ionic conductivity) will also be mentioned.

Keywords: Intercalation of kaolinite, Facile preparation, Multiple functional properties.

1. INTRODUCTION

The diverse reactions and widespread distribution of clay minerals have piqued the interest of investigators since prehistoric times, making them a common component of the earth's surface layers [1]. These minerals can be classified into categories based on layer type and interlayer species, including Kaolinite, Pyrophyllite, Smectite, Mica, and Chlorite [2]. In addition, clay minerals always adopt lamellar structures with variable intercalated water molecules and/or other agents. Hence, due to their high surface area and ion-exchange characteristics, clay minerals are widely used in the field of ceramics, paper industries, oil drilling, catalysts or catalyst supports, pharmaceuticals, adsorbents and so on [3-5]. Comprehensive reviews of the classification and utilization of these clay minerals were provided by Bergaya and Lagaly [6].

Kaolinite (abbr. as K), a clay mineral with the theoretical formula $Al_2Si_2O_5(OH)_4$, is widely abundant across the globe. It can be found in or near soils, sediments, and sedimentary rocks. This mineral serves as a significant raw material in various industries, particularly as a paper filler and coating pigment [7, 8]. To enhance its performance, kaolinite is often subjected to physical or chemical treatment to modify its natural state. Over the years, there has been continuous interest in the preparation, surface treatment, modification, structural characterization, and thermal stability of intercalated kaolinites [9, 10]. Several decades ago, K. Wada made a discovery that cations and anions can permeate between the silicate layers of kaolinite group minerals, potentially forming a unimolecular layer of the ionic complex [11]. Subsequently, the preparation of kaolinite-potassium acetate intercalated compound was also reported [12]. In the next time, a large kind of intercalated kaolinites with different intercalated guest molecules were prepared and then were characterized by means of FT-IR, Raman, TG/DTA and so on [13-16]. Recent review provided by Zhang *et al.* [17] summarized the typical synthetic procedures and conditions, characterization methods of kaolinites, and the subsequent reviews presented by Frost *et al.* summarized the vibrational spectrum as well as the thermal behavior of pure/intercalated kaolinites [18, 19]. However, the investigations that focused on multiple physical properties of intercalated kaolinites, such as dielectricity even ferroelectric properties, was negligible for quite a long time. In fact, the pursuit of novel and high performance functional materials will never stopped with the progress of human beings' history, namely, developing the novel and intriguing functionalities from old materials are strongly needed and are still remaining a lot of challenges.

Recently, special efforts have been put into this important part of intercalated kaolinites, namely, the multiple functional properties of this material become more and more attractive. For instance, N. Bizaia and co-workers [20] reported an efficient catalyst used porphyrin-kaolinite for oxidation reactions of new biomimetic catalysis showing high conversion ratio and complete selectivity for the specific product, and In the investigation conducted by Kumrić *et al*., a potential application of modified kaolinite as an economical and

*Address correspondence to this article at the Institute of Functional Nano&Soft Materials (FUNSOM), Jiangsu Key Laboratory for Carbon-Based Functional Materials & Devices, Soochow University, Suzhou 215123, Jiangsu, PR China; E-mail: haoyang@suda.edu.cn

efficient adsorbent was explored. This adsorbent showed promising capabilities for achieving highly efficient removal of divalent heavy metals from aqueous solutions, making it suitable for the treatment of heavy-metal contaminated waste waters [21]. Besides, a new luminescent hybrid materials based on kaolinite covalently grafted by terbium picolinate was reported by Faria *et. al.* [22] which showing stronger characteristic emission than the isolated complex, and then in an important review by Suzuki, the intercalation of kaolinite with ortho- and para-nitroanilines, carried out by Takenawa and co-workers, [23] was summarized [24]. This intercalation resulted in the exhibition of second nonlinear optical properties, attributed to the asymmetric environment of the interlayer region of kaolinite. In short, intercalated kaolinites appear as promising materials for many applications due to their specific properties and the researches focused on this part are also gradually began to study till now.

In order to systematically and deeply investigate the versatile properties of intercalated kaolinites, we chose several kinds of typical molecules as intercalation agents and these agents can be attributed to three categories qualitatively, that is, I) the intercalant that has been widely studied, such as dimethyl sulfoxide, urea and potassium acetate, used for comparison with the common preparation methods and discovering new functional properties, II) homologous series or analogue, including aminopyridine derivatives as well as ethanolamine and ethanediol, to examine the effects of small changes of substituent, III) organic acid molecules which may mainly focus on the proton conductivity based on these intercalated kaolinite compounds since all of these molecules are good candidates for proton donor/acceptor. What's more, the novel preparation method we proposed can be tested and verified if it is applicable and practical via utilizing categories II&III that have been studied rarely and will be mentioned in the next part.

In this review article, we summarize our recent results on facile preparations of twelve intercalated kaolinites compounds with organic molecules or fatty acid salt as intercalated agents (the detailed intercalated compounds within the corresponding intercalated agents are listed in Table **1**) and propose a cost-effective strategy for highly-efficient preparation of intercalated kaolinite compounds under mild condition. In addition, the multiple physical properties (*e.g.* dielectricity, ferroelectricity and ion conductivity) will also be discussed to throw out a minnow to catch a whale.

2. PREPARATION METHODOLOGY OF INTERCALATED KAOLINITES

Kaolinite, a 1:1 phyllosilicate with a lamellar structure, possesses consecutive layers that are connected through weak hydrogen bonding interactions and van der Waals forces. These interactions occur between the aluminol groups of the octahedral sheet on one side and the siloxane rings of the tetrahedral sheets on the other side [33, 34]. The siloxane layer consists of SiO_4 tetrahedral arranged in a hexagonal pattern. The bases of the tetrahedral are approximately co-planar, and the apical oxygen atoms are linked to the second layer containing aluminum ions and OH groups, forming the gibbsite-type layer [35]. As a result, intercalation which involves the insertion of guest molecules into the inter-lamellar

Table 1: Various Intercalated Agents used in Compounds 1-12

Compound	Intercalated Agent	Abbr. as	References
1	Dimethyl sulfoxide	K-DMSO	25
2	Urea	K-Urea	
3	Potassium acetate	K-KAc	26
4	Ethanediol	K-EG	27
5	Ethanolamine	K-EOA	
6	2-aminopyridine	K-2-APy	28
7	3-aminopyridine	K-3-APy	
8	4-aminopyridine	K-4-APy	
9	HCl&4-aminopyridine	K-4-APy-HCl	29
10	2-Picolinic acid	K-2-Pa	30
11	L-alanine	K-Ala	31
12	KH_2PO_4	K-KDP	32

spaces of kaolinite, can be achieved [36-40]. However, the intercalation process of kaolinite is more difficult than those layered clay minerals (*e.g.* Montmorillonite [41]), because of the strongly interlayer interactions.

The earlier researches focused on the preparation of intercalated kaolinite were done by Weiss *et. al.* [42] in the nineteen sixties, however, the detailed intercalation process and mechanism was still obscure due to the technical limitation at that time. And then, Frost and co-workers did a great job of explaining and illustrating the principles through practical examples, namely, they explored the role of various intercalant as well as water in the intercalation process, such as specifying various binding modes in intercalated kaolinites based on IR spectra, [43] investigated some key factors in preparation process, such as concentration of intercalant, reaction temperature, and then found the best condition for each easily-intercalated agent [44]. Meanwhile, they analyzed the vibrational spectroscopy, thermal behavior of intercalated kaolinite using DRIFT, Controlled rate thermal analysis (CRTA) techniques [45]. In short, the basic principles of preparing kaolinite intercalated compounds was achieved and then large quantity of new intercalated kaolinites were prepared using their condition [46].

Generally, some organic compounds (such as formamide [47], hydrazine [48], potassium acetate [49], dimethyl sulfoxide (DMSO) [50]), with small molecular size and large dipole moments (high polarity), can be intercalated directly into kaolinite by means of either the liquid phase intercalation (for instance, intercalated from concentrated aqueous solution) or the melting process [51]. Besides, other compounds, such as glycol [52], pyridine-carboxylic acids [53] and fatty acid salt [54], cannot intercalate directly into kaolinite, but they can be introduced by displacement of a previously intercalated compound, via an exchange reaction. It should be noted that all above intercalation processes utilized conventional intercalated methodology need a long time, generally about several days even several weeks to reach the maximum intercalation rate [55-57], which means high cost and low efficiency.

We proposed a facile and efficient strategy for the rapid preparation of intercalated kaolinites with small organic molecules under mild conditions using an autoclave, aiming to improve intercalation conditions and enhance efficiency. As a result, the reaction time was significantly reduced to just a few hours. As Figure **1c** shown, the DMSO molecules inserting into the interlayers of kaolinite will expand lamellar space. Actually, the whole intercalation is an entropy and volume reducing process. Increasing the pressure in a sealed reactor can reasonably promote the intercalation reaction. In fact, undertaking the intercalation reaction of kaolinite with small organic molecules at much higher pressure using a Parr bomb results in reaching the maximum intercalation rate in less time [58]. As summarized in Table **2**, we can obviously judge the advantage of method we proposed in practical application.

In addition, the intercalation processes of some large size molecules and/or other indirectly intercalated agents inserted into kaolinite are very difficult. Generally, a so-called exfoliation method which utilized intercalated kaolinite such as methoxy-modified kaolinite as precursor is employed [63, 64] and/or form various nanomaterials with multiple functionalities [65-67], however, it always takes more complicated routes compared to aforementioned method. Thus, these agents also can adopt this methodology, namely, utilized the K-DMSO hybrid compound as a precursor compound to intercalate, obtaining an efficient result with high intercalated ratio.

Table 2: Comparison of Required time of Preparing Typical Intercalated Kaolinite Compounds in Different Methods

Compound Name	Intercalated Agent	Preparation Method	Required Time / h	Ref.
K-DMSO	Dimethyl sulfoxide	Solution immersing method	72	59
		Autoclave hydrothermal method	6	25
K-Urea	Urea	Aqueous suspension method	192	60
		Autoclave hydrothermal method	6	25
K-KAc	Potassium acetate	Saturated solution shaken method	80	49
		Intercalated with K-DMSO as precursor	10	26
K-N_2H_4	Hydrazine	Solution stirring method	80	48
K-NMF	N-methyl formamide	Solution stirring method	96	61
K-Aca	acetamide	melt intercalation method	168	62

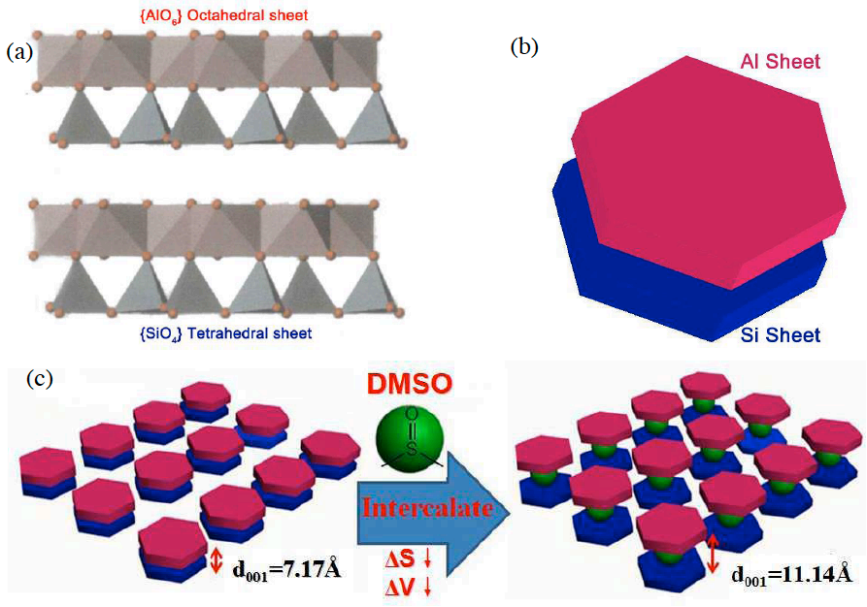

Figure 1: (**a**) Molecular structure of raw kaolinite and Schematic illustration of (**b**) the aluminol groups sheet and siloxane sheet of kaolinite and (**c**) the intercalated process of kaolinite inserted with DMSO.

3. INTERLAYER SPACE AND INTERCALATED RATIOS

In contrast to the distinct increase in interlayer space observed with various intercalated molecules, the insertion of intercalated agents into the interlayer of raw kaolinite generally does not significantly impact the layered structure of the host aluminosilicate (see Table **3**). As displayed in Figure **2**, the distinct 2θ values corresponding to the interlayer distance of various intercalated and raw kaolinites can be reflected *via* the powder XRD characterization. The characteristic (001) reflection in the diffraction profile of raw kaolinite, typically represented by the peak at 2θ = 12.34°, allows for the calculation of the interlayer distance between silicate and gibbsite sheets (d(001)), which is determined to be 7.17 Å [68]. When various intercalated agents are introduced into the space between the silicate and gibbsite sheets, this characteristic (001) reflection shifts towards lower angles.

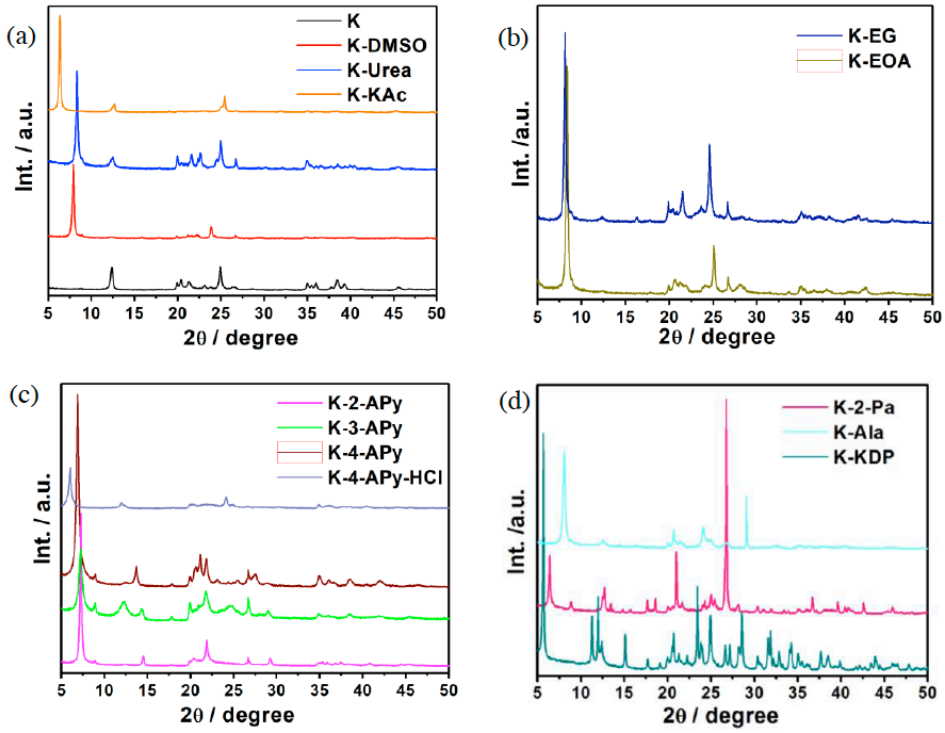

Figure 2: Powder XRD patterns of the samples (**a**) Raw kaolinte and compounds **1**-**3**, (**b**) **4** and **5**, (**c**) **6**-**9** and (**d**) **10**-**12** in the 2θ range of 5-50°, respectively. (Reproduced from Ref. 25-32 with kind permission of publisher of papers).

By utilizing Equation (1) [69], the estimation of intercalation efficiency can be derived from the relative intensities of the "unchanged" and "expanded" (001) diffraction peaks. This estimation is based on the mass fraction of the intercalated material, which can be determined from the intensity of the (001) diffraction peak.:

$$I.R. = \frac{Int.(001)\ of\ intercalated\ Kaolinite}{Int.(001)\ of\ intercalated\ Kaolinite + Int.(001)\ of\ raw\ Kaolinite} \quad (1)$$

Intercalation ratio (*I.R.*) of compounds **1**-**12** are also listed in Table **3**. It should be noted that almost all of the intercalation ratios are higher than 90%, namely, the simple approach we proposed is very efficient.

Table 3: The Distinct Interlayer Distances and Intercalation Ratios of Intercalated Compounds 1-12

Compound	Interlayer Distance (Å)	Intercalation Ratio (%)
1	11.14	97
2	10.61	91
3	14.20	92
4	10.85	98
5	10.57	99
6	11.98	92
7	12.10	74
8	12.99	93
9	14.41	86
10	13.50	75
11	10.91	94
12	15.50	90

Note: The interlayer space of raw kaolinite is calculated as 7.17 Å based on PXRD data [57].

4. PROPERTIES

In general, functional properties are very important for either natural or artificial materials since they deserve to be utilized practically only if they possess any kind of properties. And as such, more and more researches are focused on the properties of materials whether they are 'withered' or new. For the traditional kaolinite, there are just some sporadic reports on specific properties till now, so there still remain a lot of interesting functional properties that need to be systematically studied and will be discussed in detail in the next part.

4.1. Dielectric Properties for 1-8

Dielectric material is a kind of important functional electronic material since it can be applied in the field of microelectronics, electric power systems, storage and sensor [70]. Rarely have studies been reported on the dielectric properties of intercalated kaolinite compounds, with most research to date primarily focusing on other aspects. The initial report on the dielectric properties of kaolinites intercalated with various small molecules, such as urea, potassium acetate, and N-methylformamide, was conducted by K. Orzechowski and colleagues [71]. They compared the difference of dielectric constant and loss between as-prepared and heated conditions in the selected frequency region for these intercalated kaolinite. Typically, as Table **4** shown, the dielectric permittivity of K-Urea and K-NMF is just a little larger than raw kaolinite, whereas for the K-KAc, it is more than 5 times than kaolinite. Unlike K-Urea and K-NMF, which bond with both sheets of kaolinite, it is evident that potassium acetate molecules interact exclusively with the gibbsite sheet. This implies that dipolar molecules have the potential for movement within a relatively spacious interlayer region. After heating, all the permittivity considerably decrease due to loss of interlayer water and those values are much similar to the value observed in kaolinite.

In our works, the temperature-dependence and frequency-dependence dielectric behaviors of the intercalated kaolinites are fully experimentally investigated, besides, the dielectric relaxation processes and detailed relaxation mechanism are also be very concerned.

4.1.1. Dielectric Constant and Loss

Figure **3** displays the frequency-dependent dielectric constant and loss for compounds **1** and **2** over the range of 1-10^9 Hz. In the low-frequency range (1-10^3 Hz), the dielectric constant decreases rapidly with increasing frequency for both compounds, indicating the presence of a slow dielectric relaxation process. Notably, the plots of dielectric loss versus frequency exhibit distinct characteristics between the two intercalated compounds. Unlike to compound **1,** Compound **2** shows broad maximum peaks, illustrating the significant influence of the intercalated molecule on the dielectric properties of the compound. There are typically four different dielectric relaxation mechanisms, each associated with a characteristic relaxation frequency. Electronic transitions or molecular vibrations contribute to dielectric relaxation at frequencies above 10^{12} Hz, while dipole motion or ionic polarization occurs in the frequency range of 10^2-10^{10} Hz. Consequently, the observed dipole motion of intercalated molecules in the intercalated kaolinites gives rise to the dielectric relaxation in the low-frequency region of 1-10^3 Hz.

Table 4: Summary of the Dielectric Constant and Loss Obtained in K, K-Urea, K-NMF and K-KAc in Different Conditions. (Reproduced from Ref. 71 with Kind Permission of the Elsevier, Publisher of *Journal of Physics and Chemistry of Solids*)

	ε′ (10 kHz)	ε″ (10 kHz)	ε′ (100 MHz)	ε″ (100 MHz)	ε′ (4 GHz)	ε″(4 GHz)
K	4.29	1.08	2.14	0.03	2.11	0.13
K (after 400 ℃)	3.40	0.52	2.01	0.06	1.91	0.12
K-Urea	4.71	1.73	2.44	0.04	2.41	0.17
K-Urea (after 400 ℃)	3.22	0.38	2.16	0.05	2.12	0.17
K-NMF	6.08	2.36	3.31	0.06	2.99	0.20
K-NMF (after 400 ℃)	3.95	0.54	2.28	0.05	2.34	0.16
K-KAc	26.0	79.8	3.06	0.39	2.73	0.25
K-KAc (after 400 ℃)	15.7	59.0	2.92	0.11	2.68	0.18

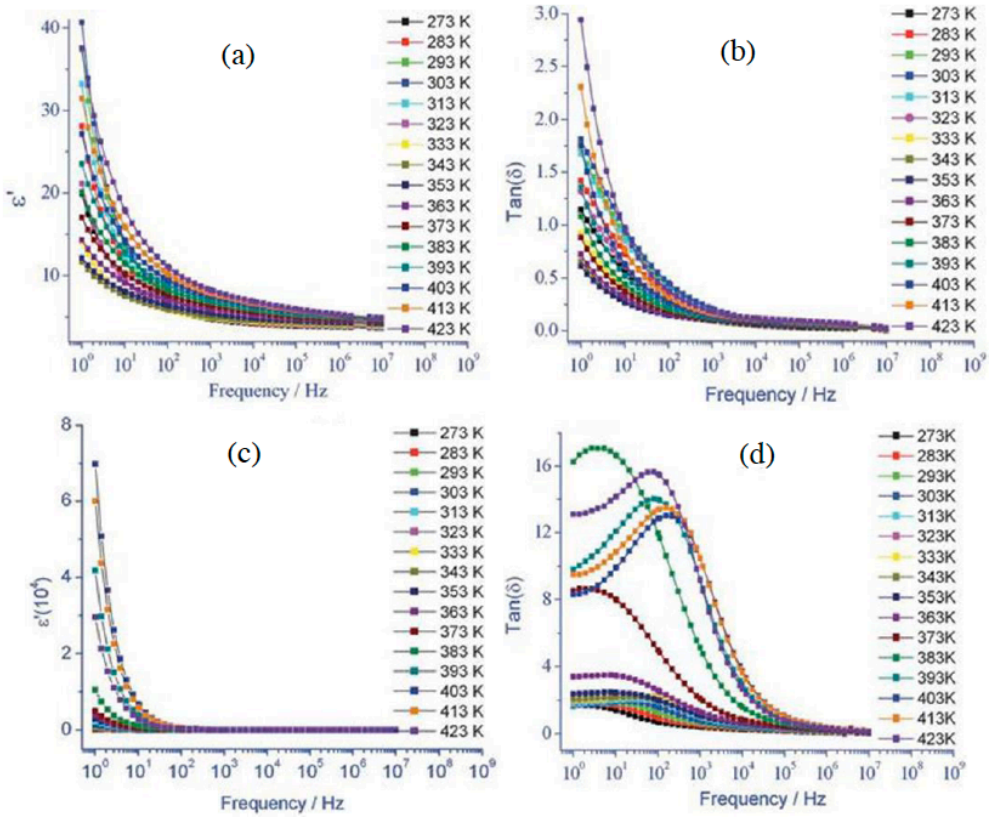

Figure 3: Frequency dependences of *ε′* and *tan(δ)* in the temperature range of 273-423 K for compounds (**a**, **b**) **1** and (**c**, **d**) **2**, respectively. (Reprinted from Ref. 25 with permission of the Royal Society of Chemistry, Publisher of *Journal of Material Chemistry*).

Figure **4** depicts the temperature dependence of the dielectric constant and loss within the frequency range of 1-29 Hz. Both of compounds **1** and **2** exhibit a dielectric anomaly around 300 K, resembling the behavior of H2O. This anomaly likely arises from the absorption of a small amount of moisture by the powdered sample pellets from the surrounding moist air [72]. When comparing the dielectric behavior of compounds **1** and **2** in the low-frequency region, two significant differences become apparent:

I) Compound **2** displays an additional dielectric anomaly in its temperature-dependent dielectric spectroscopy, with a maximum centered around ~402

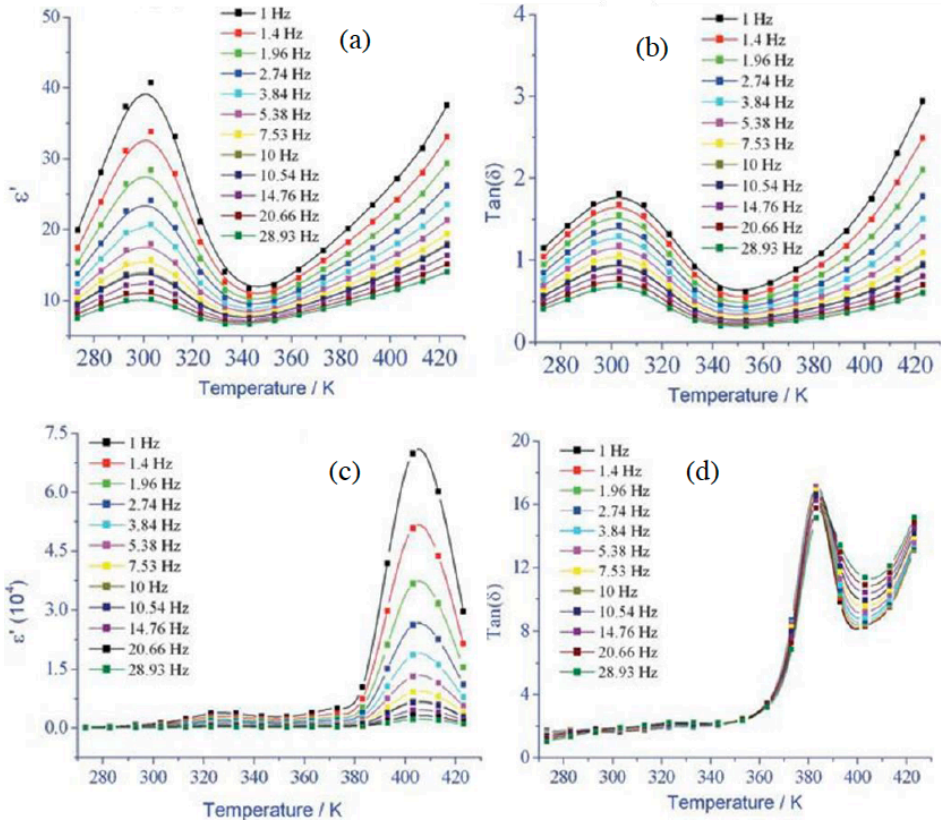

Figure 4: Plots of temperature-dependence of *ε'* and *tan(δ)* in the frequency range of 1-29 Hz for compounds (**a**, **b**) **1** and (**c**, **d**) **2**, respectively. (Reprinted from Ref. 25 with permission of the Royal Society of Chemistry, Publisher of *Journal of Material Chemistry*).

K. This anomaly is associated with the collective movement of intercalated urea molecules [71] or a ferroelectric-to-paraelectric transition. In contrast, for compound **1**, both the dielectric constant and loss exhibit a monotonic increase as the temperature rises up to 423 K. It is possible that compound **1** may have a dielectric anomaly at higher temperature, but we cannot verify this point as the DMSO molecules inserted in kaolinite are released above 409 K.

II) The dielectric constant for compound **1** remains below 40, while compound **2** reaches a value of 10^4.

In the frequency range of 1-10^4 Hz, compounds **4** and **5** exhibit a rapid decrease in ε' values with increasing frequency. This decrease can be attributed to the inability of dynamical dipole motion to keep pace with the switching of the applied ac electric field at higher frequencies (f > 10^4 Hz). The frequency-dependent plots of *tan(δ)* for compounds **4** and **5** exhibit distinct characteristics. For compound **4**, there are two broad maxima observed in the *tan(δ)-f* plots within the temperature range of -95 to -50 °C. Similarly, compound **5** displays a broad maximum in the *tan(δ)-f* plots within the temperature range of -80 to 80 °C (refer to the inset of Figure **5d**). Upon heat treatment, the position of the peak in the *tan(δ)-f* plot for both compounds **4** and **5** shifts toward higher frequencies, indicating the typical feature of thermally assisted dielectric relaxation.

As shown in Figure **6**, the dielectric permittivity of compounds **6**-**8** exhibits a rapid decrease with increasing frequency within the range of 1-10^4 Hz. This decline indicates that the dynamical motion of dipoles cannot keep up with the rapid switching of the applied electric field at frequencies higher than 10^4 Hz for the intercalated compounds. When beyond 10^6 Hz, the dielectric permittivity remains nearly constant. As the temperature rises, the intercalated compounds **6**-**7** show a noticeable dielectric dispersion in the low-frequency range. This dispersion is attributed to the increased mobility of the intercalated molecules, which is further supported by the observation of larger dielectric loss at higher temperatures. Compound **8** exhibits two peaks in the dielectric loss plot: one below 10^4 Hz within the temperature range of 20-160 °C, and another broad peak in the 10^4 - 10^5 Hz range below 80 °C. Interestingly, the shape of the curves for compounds **6**-**8** closely resembles that of raw kaolinite when the applied ac field frequency is below 10^2 Hz.[25] For all three compounds, the position of the peak in the *tan(δ)* versus frequency plot shifts toward higher frequencies as the temperature increases, demonstrating the characteristic behavior of thermally assisted dielectric relaxation. Similar to compounds **1** and **2**, the observed dielectric relaxation in the

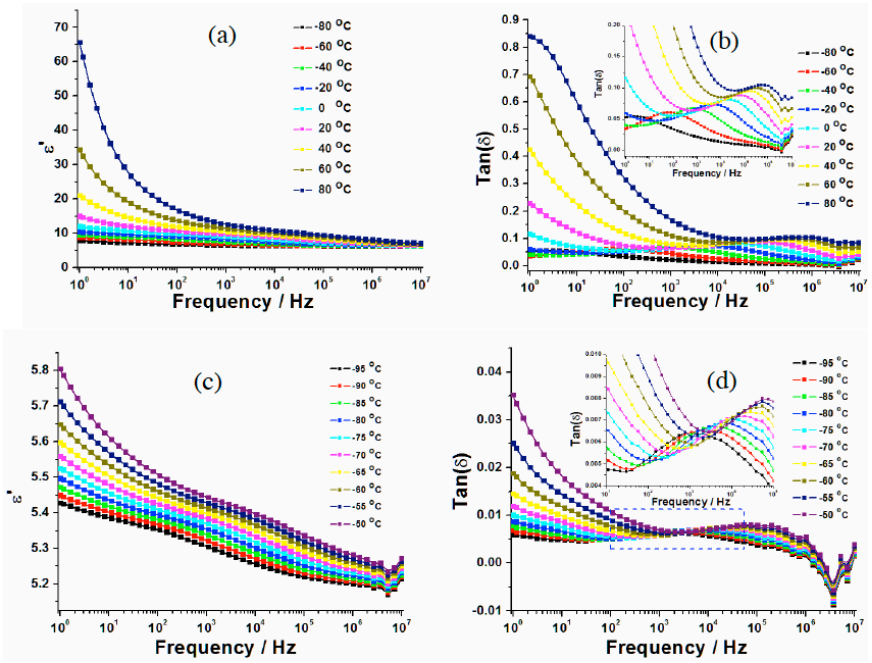

Figure 5: Frequency dependences of ε′ and tan(δ) for (**a**, **b**) **4** in the range -95-50 °C (**c**, **d**) **5** in the range of -80-80 °C. (Reprinted from Ref. 28 with permission of the Royal Society of Chemistry, Publisher of *Dalton Trans.*).

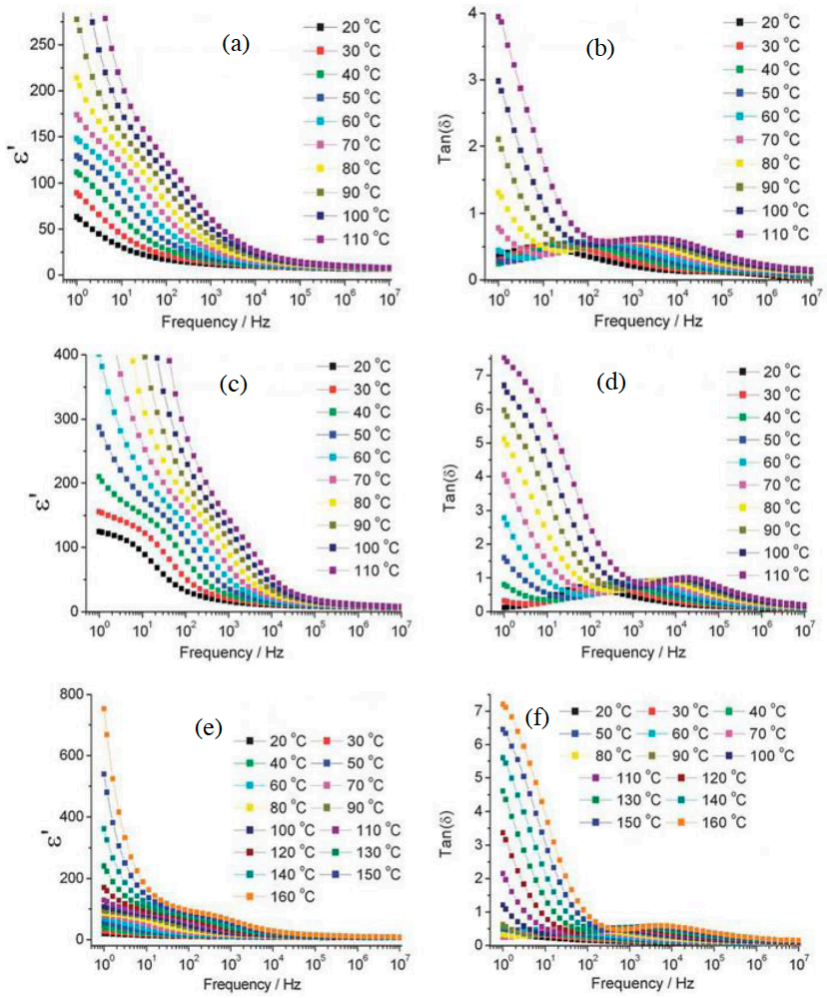

Figure 6: Frequency dependences of *ε′* and *tan(δ)* for (**a**, **b**) compound **6** in the range 20-110 °C (**c**, **d**) **7** in the range 20-130 °C and (**e**, **f**) **8** in the range of 20-180 °C. (Reprinted from Ref. 26 with permission of the Royal Society of Chemistry, Publisher of *RSC Advance*).

low-frequency region for compounds **4**-**8** also arises from the molecular-dipole motion of the intercalating molecules.

By comparison of two analogues separately, it is worth noting that even minor change of intercalated agent molecule (*e.g.* position of the substituted group) will lead to obvious difference of specific properties of intercalated kaolinites, indicating the importance of systematical investigation.

4.1.2. Dielectric Relaxation Behaviors

Further analysis is conducted to gain deeper insights into the dielectric relaxation behaviors of the aforementioned intercalated compounds. To achieve this, we utilize the following empirical Arrhenius relationship to assess the macroscopic relaxation time:

$$\tau = \tau_0 \exp(\frac{E_a}{k_B T}) \quad (2)$$

Where $\tau = 1/f_{max}$ and f_{max} is the frequency at maximum of *tan*(δ)-*f* plot at elevated temperature; τ_0 is the characteristic macroscopic relation time, E_a refers to activation energy/potential barrier. The best fitting results using Eqn. *(2)* are listed in Table **5**.

The behavior of most dielectric materials differs from the Debye response, necessitating modifications to the empirical expression that represents the Cole-Cole plot. One proposed modification, introduced by Cole and Cole [73], is given by:

$$\varepsilon^* = \varepsilon_\infty + \frac{\varepsilon_0 - \varepsilon_\infty}{1 + (i\omega\tau)^{1-\alpha}} \quad (3)$$

Here, the static permittivity ε_0 and the permittivity at theoretically infinitely high frequencies ε_∞ are important parameters in the context of the discussed intercalated compounds. Additionally, the relaxation time τ and the parameter α are associated with the dispersion of relaxation processes within the range of $0 < \alpha < 1$.

As shown in Figure **8**, the Cole-Cole plots depict the relaxation process for these intercalated compounds at selected temperatures. The plots of ε''-ε' were fitted to obtain the corresponding parameters ε_0, ε_∞, and α, which are summarized in Table **6**. It is noteworthy that the fitted ε_∞ parameter closely approximates the dielectric constant at higher frequencies ($f > 10^6$ Hz) for

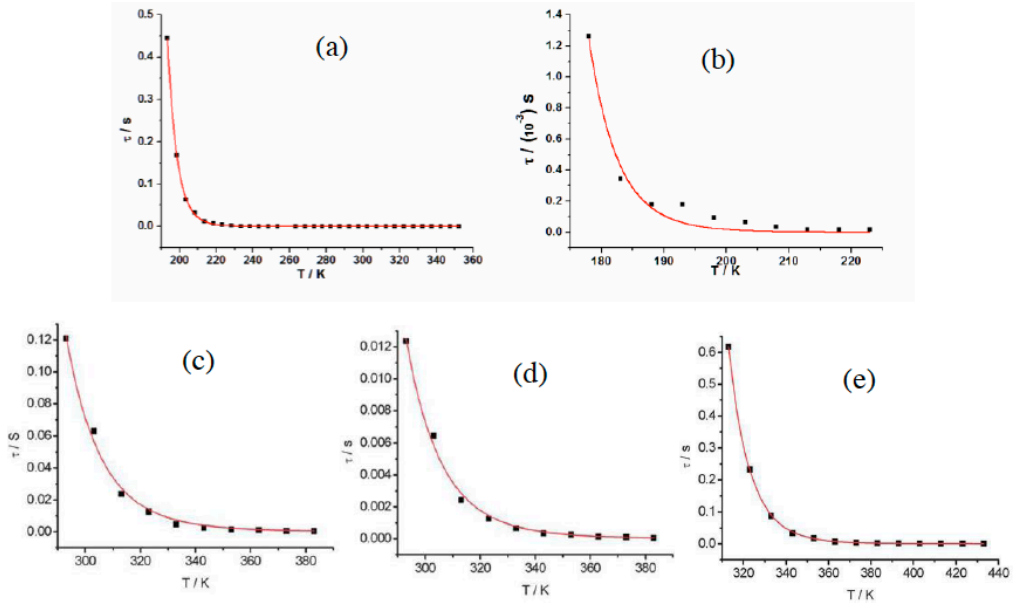

Figure 7: Plots of τ versus T for compounds (**a**) **4**, (**b**) **5**, (**c**) **6**, (**d**) **7** and (**e**) **8**, respectively. (Reprinted from Ref. 26&28a with permission of the Royal Society of Chemistry).

Table 5: τ_0 and E_a Parameters Obtained from the Best Fits for Compounds 4-8

Compound	τ_{01} / s	τ_{02} / s	E_{a1} / kJ/mol	E_{a2} / kJ/mol
4	$6.8(6)\times10^{-18}$	/	62.2(3)	/
5	$1.5(7)\times10^{-20}$	/	57.5(8)	/
6	$3.6(4)\times10^{-9}$	/	31.0(7)	/
7	$7.6(0)\times10^{-8}$	/	19.4(7)	/
8	$2.0(4)\times10^{-7}$	$1.6(3)10^{-7}$	28.6(2)	18.1(6)

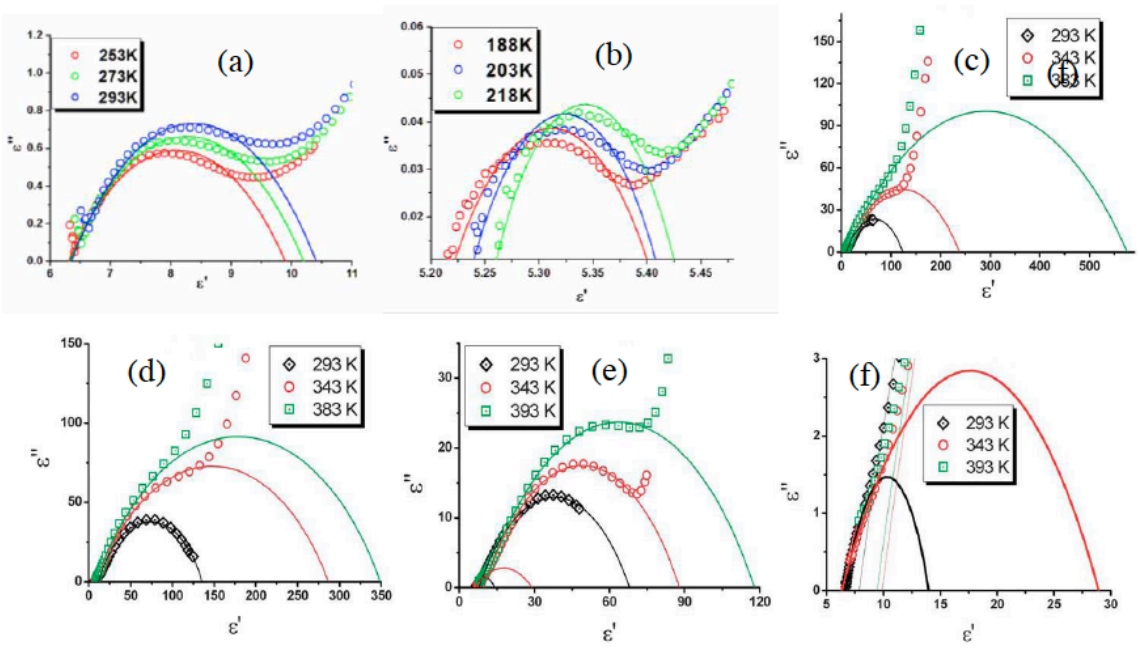

Figure 8: Plots of *ε'' versus ε'* at selected temperatures for compounds (**a**) **4**, (**b**) **5**, (**c**) **6** and (**d**) **7**, (**e**) and (**f**) **8**, respectively (Open circles: experimental data; curves: theoretically reproduced using Eqn. (3)). (Reprinted from Ref. 26&28a with permission of the Royal Society of Chemistry).

Table 6: ε_0, ε_∞ and α Parameters Obtained from the Best Fits for Compounds 4-8, Respectively

Temperature	ε_0	ε_∞	α
4			
253 K	9.89	6.305	0.59
273 K	10.2	6.320	0.58
293 K	10.4	6.348	0.55
5			
188 K	5.414	5.207	0.54
203 K	5.419	5.227	0.47
218 K	5.435	5.249	0.43
6			
293 K	773.8	10.5	0.40
353 K	754.0	12.1	0.33
383 K	866.2	12.1	0.33
7			
293 K	48.0	6.0	0.41
353 K	48.7	6.2	0.35
393 K	52.0	6.2	0.31
8			
293 K	73.6 (262.9)*	5.8 (15.3)	0.51 (0.56)
353 K	83.3 (186.2)	6.6 (17.4)	0.48 (0.51)
393 K	120.2 (211.5)	6.6 (16.6)	0.49 (0.44)
*Note: Compound **8** shows two-step relaxation processes and possesses two sets of relaxation parameters.			

each intercalated compound. Furthermore, the fitted α parameters deviate significantly from zero, indicating a departure of the relaxation process from the Debye dielectric response for all the aforementioned intercalated compounds.

4.2. Ferroelectric Properties for 1-2

Figure **9** displays the characteristic ferroelectric hysteresis loop exhibited by these two intercalated kaolinite compounds. In contrast, the dried raw kaolinite demonstrates an almost linear P-E relationship, accompanied by a very small symmetric shuttle-shaped loop. It is worth noting that in some cases, lossy dielectrics can also exhibit a hysteresis loop during electrical hysteresis measurements. Such dielectric hysteresis loops are typically associated with higher leakage currents, as the dielectric loss is directly proportional to conductivity. During our dielectric hysteresis loop measurements for compounds **1**-**2**, remarkably low leakage currents (~10^{-6} A•cm^{-2}) were observed, confirming that the observed hysteresis loops are indeed a result of ferroelectricity. Figure **9d** illustrates the leakage current as a function of the applied electric field for compound **1**. The occurrence of a ferroelectric hysteresis signifies the reversal or switching of the macroscopic polarization in the ferroelectric material. This reversal at the macroscopic level indicates a corresponding reversal at the local, microscopic level. The overall polarization in a dielectric material encompasses four distinct dielectric mechanisms: electronic, atomic, orientation or dipolar, and ionic polarization. Electronic polarization arises when an electric field displaces the nucleus relative to the surrounding electrons in neutral atoms. Atomic polarization occurs when neighboring positive and negative ions experience deformation under the influence of an applied electric field. Both electronic and atomic polarizations give rise to induced dipole moments based on the polarizabilities of the atoms or molecules. Permanent dipole moments result from an imbalance in electron sharing among the atoms of a molecule. Ionic polarization involves ionic conductivity and interfacial or space charge polarization.

In the case of compounds **1** and **2**, the microscopic polarization reversal under the applied electric field is comprehensible due to several factors. Firstly, there are weak intermolecular hydrogen bond interactions and van der Waals forces between the guest molecules and the inorganic host. Secondly, the average occupied volume per guest molecule is estimated to be approximately 141.08 $Å^3$ for DMSO and 157.71 $Å^3$ for urea in their corresponding intercalation compounds. These volumes are significantly larger than their van der Waals volumes (118.41 $Å^3$ for DMSO and 73.4 $Å^3$ for urea, respectively). As a result, it is possible that the guest molecules occupying the interlayer space of the inorganic host, have sufficient space for relative molecular displacements, similar to the observations in the molecular ferroelectric crystal of thiourea or the flipping of molecules [76]. It should be noted that the actual alignment pattern of the guest molecules in the interlayer of kaolinite, as well as available crystal structure information for the intercalated hybrids, still requires further investigation through molecular dynamics simulations, which is currently in progress.

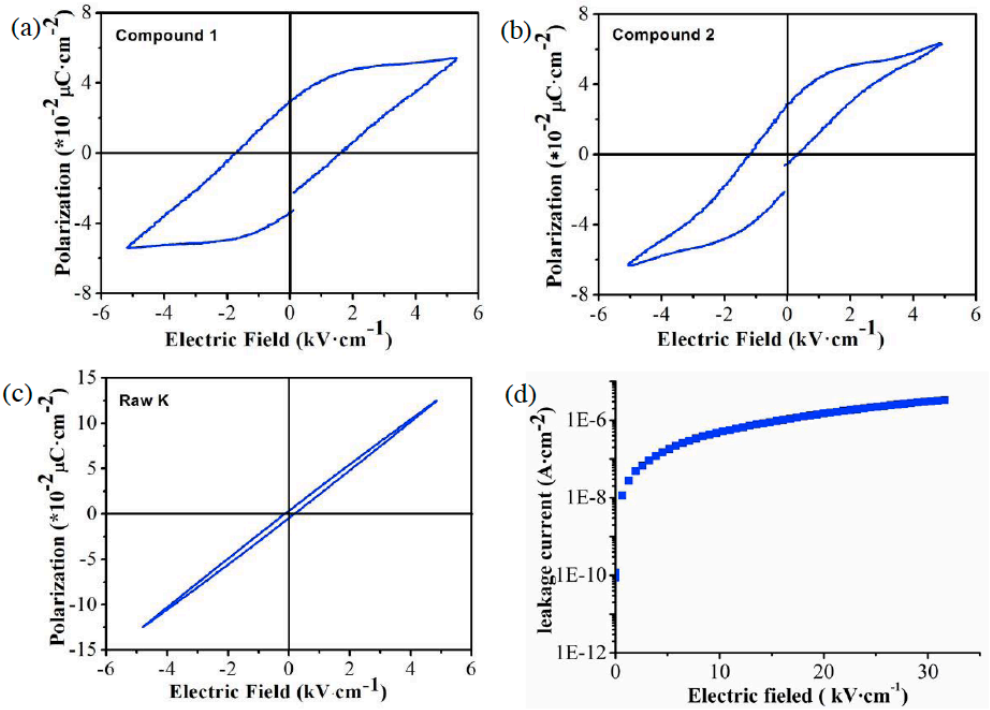

Figure 9: (**a**), (**b**) and (**c**) P-E hysteresis loops of intercalation compounds **1** and **2** and raw kaolinite under selected electric field (*f* = 16.7 Hz) at room temperature and (**d**) the leakage current *vs.* electric field for **1**. (Reprinted from Ref. 25 with permission of the Royal Society of Chemistry).

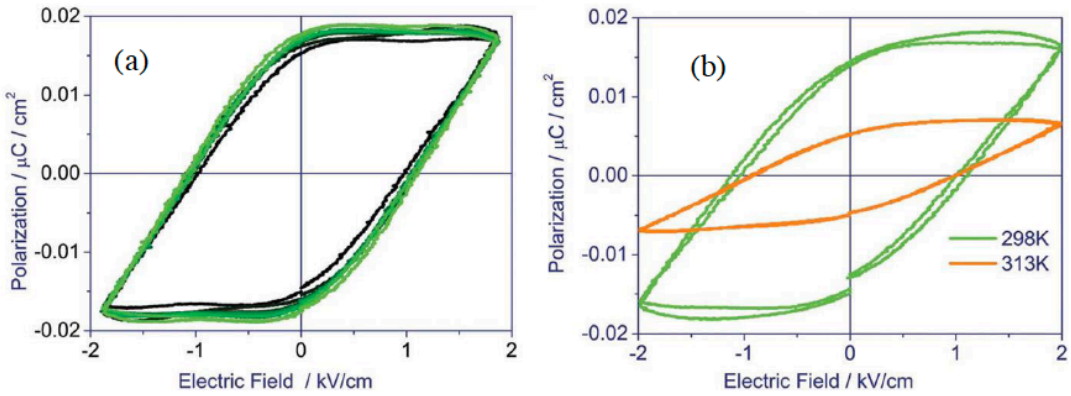

Figure 10: Plots of P *v.s.* E of K-EG-cg at 16.7 Hz with (**a**) ambient temperature and (**b**) different temperature, respectively. (Reprinted from Ref. 27b with permission of the Royal Society of Chemistry).

A novel ferroelectric compound based on intercalated kaolinites, namely kaolinite covalently grafted with ethylene glycol (abbr. as K-EG-cg), has recently been proposed [27b]. This compound exhibits inherent ferroelectric properties, characterized by a spontaneous polarization (PS) of approximately 0.018 μC cm^{-2}, a remanent polarization (Pr) of around 0.015 μC cm^{-2}, and a coercive field (EC) of approximately 1.045 kV cm^{-1} at room temperature. The presence of clear ferroelectric hysteresis loops at various temperatures is illustrated in Figure **10**. It is noteworthy that the P-E measurements indicate the reversibility of macroscopic polarization in K-EG-cg, primarily attributed to the circular motion of the covalently grafted ethylene glycol (EG) molecules.

4.3. Ion Conductivity for 3 and Proton Conductivity for 9, 10, 11 and 12

4.3.1. Ion Conductivity

The first report of ion conductivity of intercalated kaolinites was investigated by S. Letaief and co-workers [77], they prepared nanostructured hybrid kaolinite intercalated with a series of imidazolium derivatives and measured the temperature-dependence electrical conductivity.

Apart from the dielectric property which has mentioned above, we additionally investigate the ion conductivity of compound **3**. Figure **11a** presents the Nyquist plots for compound **3** at different temperatures. Typically, the resistance of a material can be directly inferred from the diameter of the semicircle in a Nyquist plot. In the relatively low temperature range (below 373 K), the plots appear as nearly straight lines, suggesting the presence of an infinite semicircle. This characteristic indicates a high resistance of the material. As the temperature increases, the Nyquist plots exhibit a visible semicircle shape, with the diameter of the semicircle decreasing. This decrease signifies an increase in ionic conductivity at higher temperatures, attributed to thermally assisted ionic motion. Furthermore, Figure **11b** provides close-up views of the high-temperature regions of the Nyquist diagrams (413, 418, and 423 K). In these views, a distinct semicircle appears at high frequencies, followed by a small tail at low frequencies caused by the electrode effect. This observation suggests that the conductivity primarily arises from alternating current (ac) impedance rather than direct current (dc).

Compound **3** exhibits ionic conductivity, which can be attributed to two categories of ion movement. The first category involves the migration of basic ions within the layers of kaolinite, known as intrinsic conduction. The second category involves the movement of ions inserted into the interlayer space of kaolinite, such as K^+ and acetate in this case, referred to the extrinsic conduction. To gain the further insights, we also investigated the temperature-dependent impedances of raw kaolinite, as depicted in Figure **11c**. The plots of -Z'' versus Z' exhibit nearly straight lines within the temperature range from 293K to 433 K, implying that no ionic conductivity in this temperature region for raw K. Based on the above analysis, the ionic conductivity observed in compound **3** is primarily attributed to the migration of K^+ and acetate ions, which is supported by crystal structure simulations [26].

The analysis of compound **3**'s ionic conductivity involved fitting the Nyquist plots at selected temperatures. Figure **11b** presents the experimental and fitted -Z'' versus Z' plots at 413, 418, and 423 K, along with the corresponding equivalent circuit comprising R_1 and R_2, representing bulk and boundary resistances, respectively. Notably, two overlapping semicircles are observed in Figure **11b**. The fitted bulk ionic conductivity data were then plotted as ln(σT) versus 1000/T, as shown in Figure **11d**. The results indicate a significant increase in ionic conductivity across the entire temperature range, indicating

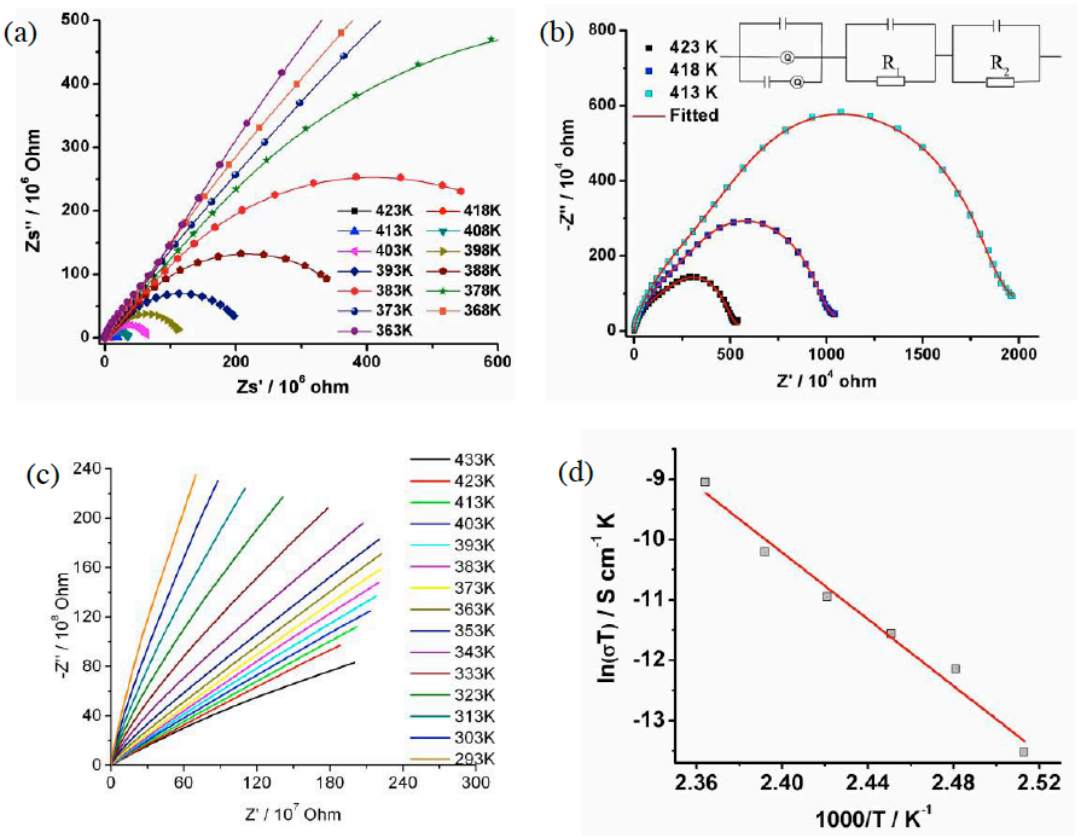

Figure 11: (**a**) Nyquist plots of compound **3** at selected temperature (363 - 423 K). (**b**) Close-up views of high temperature regions in the range of 413 - 423 K (Red lines are fitted curves, inset: Equivalent circuit diagram). (**c**) Nyquist plots of raw K at different temperature (293 - 423 K). (**d**) Plot of ln(*σT*) *versus* 1000/*T* for compound **3** (Red line is fit). (Reprinted from Ref. 26 with permission of the Royal Society of Chemistry).

enhanced mobility of interlayer ions (K^+ and acetate ions) due to thermal activation. The activation energy (E_a) was determined by fitting the ln(σT) versus 1000/T plot using Arrhenius equation,

$$\ln(\sigma T) = \ln A - \frac{E_a}{k_B T} \quad (4)$$

Here the E_a and A are activation energy and pre-exponential factor, respectively. The fitting was performed using Eqn. (4), resulting in an E_a value of 2.39 eV.

This research offers a simple approach for developing solid electrolytes for fuel cells by incorporating organic salt into lamellar minerals.

4.3.2. Proton Conductivity

Due to its potential applications in fuel cells, proton conductivity, which involves the conduction of H^+ ions, has gained significant attention [79, 80]. Kitagawa *et al*. have recently reported a series of proton-conducting materials, involved two-dimensional coordination polymers (CPs) or three-dimensional metal-organic frameworks (MOFs) [81]. For kaolinite, similar to the two-dimensional open-framework structure that possess large layered porous and capacities and effective ion exchange ability, it should be a good candidate for construction of proton conductor with good performance, however, insights focused on this area are still very few. In order to explore the real performance of intercalated kaolinites, we proposed two approaches to design four new intercalated kaolinite based proton conductor, the one is so-called 'post-synthesis', that is, synthesize the intercalated kaolinite firstly and then get kaolinite-based proton conductor after adsorbing volatile acid *via* acid-base reaction, another is directly insertion of organic acid molecules into preintercalated kaolinite (*e.g.* K-DMSO or K-KAc).

For compounds **9**, **10**, **11** and **12**, the proton conductive property under anhydrous and hydrous conditions were investigated. For instance, the impedance spectra (Nyquist plots) of compounds **9** and **10** are shown in Figure **12**. The reduction in semicircle diameter with increasing temperature indicates an increase in proton conductivity at elevated temperatures, attributed to the thermally assisted motion of protons. In contrast to compound **9**, we also examined the temperature-dependent impedances of compound **8**. Figure **12a** shows nearly straight lines

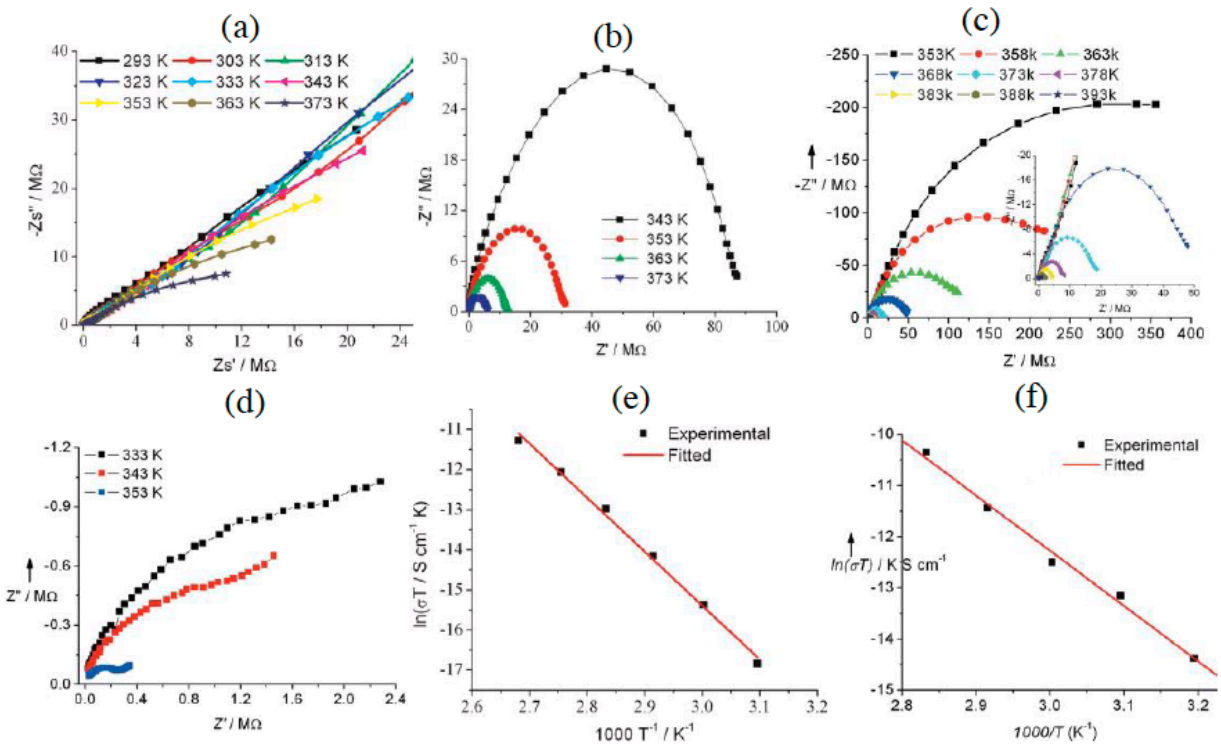

Figure 12: (**a-c**) Nyquist plots of compound **8**, **9** and **10** obtained at selected temperature. (**d**) Nyquist plot of compound **10** under 80% RH at different temperature. (**e, f**) Plot of ln(σT) *vs.* 1000/T for compound **9** and **10** (Red line is fit). (Reprinted from Ref. 29-30 with permission of Elsevier and Wiley).

Table 7: The Highest Proton Conductivity (σ) at Different Conditions and Activation Energy (E_a) Obtained from the Best Fits for Compounds 9, 10, 11 and 12, Respectively

Compound	$\sigma_{anhydrous}$ (S/cm)	σ_{RH} (S/cm)	E_a (eV)
9	3.38×10^{-8} (373 K)	/	1.159
10	1.70×10^{-10} (353 K)	1.56×10^{-7} (353 K, 80% RH[a])	1.93 (0.91[b])
11	8.31×10^{-8} (308 K)	2.10×10^{-3} (318 K, 99% RH)	0.99[b]
12	7.20×10^{-9} (358 K)	2.19×10^{-4} (293K, 100% RH)	0.618 (0.44[b])
Notes: [a]RH is respect to relative humidity, [b]The value is referred to an activation energy under 80% relative humidity at 353 K.			

within the temperature range of 293-373 K, signifying the absence of ionic conductivity in this temperature region. This observation suggests that this easy diffusive preparation strategy is very efficient for designing new intercalated compounds of kaolinite with ionic intercalants, enabling the cost-effective production of mineral-based proton conductors.

The σ value typically exhibits an increase of approximately three to four orders of magnitude when transitioning from an anhydrous state to a high relative humidity environment. This significant increase suggests that water molecules present in the interlayer spaces of kaolinite play a crucial role in the proton conduction process, as supported by previous theoretical simulations [31b]. Furthermore, when comparing the highest σ value obtained, it is comparable to those reported for ion/proton conducting materials based on MOFs or COFs [82-84], indicating the potential of intercalated kaolinite as a proton conductor.

4.4. Pollutant Adsorption for 11

Adsorption of pollutant (such as contaminants, noxious substance and exhaust gas) are also very important due to their toxicity to animals, plants and human beings [85, 86]. Due to its high abundance, local availability, non-toxicity, and chemical and mechanical stability, low costs, friendly to environment and high interlayer exchange capacity. kaolinite is a promising candidate for adsorbing such pollutants. Most recently, our investigation revealed the unique characteristic of rapid formaldehyde (HCHO) adsorption in compound **11**, which attributed to a chemical adsorption mechanism involving the rapid

formation of a Schiff base between the Alanine and HCHO within the interlayer spaces of kaolinite.

5. CONCLUSIONS & PERSPECTIVES

In summary, we have illustrated the facile strategy for controllable preparation of a series of intercalated kaolinites with small organic molecules or organic salts with high efficiency and low cost. Promoted by applied pressure in a reactor, the intercalation reaction is a process that can reduce entropy and volume for chemical reaction. The intercalated compounds show relative high intercalation ratio and are thermally stable around 100-200 °C. Additionally, all of the intercalated compounds show very abundant and intriguing physical properties, namely, compounds **1**-**5**, **7** and **8** exhibit dielectric properties with one-step or two-step dielectric relaxation behaviors, especially **1** and **2** show ferroelectricity and compounds **6**, **9**, **10**, **11** and **12** show thermal-activated ion conductivity or proton conductivity as well as compound **11** exhibits fast adsorption of HCHO. For the purpose of fabricating various devices, there has been considerable interest in a hybrid system exhibiting technologically important physical properties. The novel functionalities of dielectric properties, particularly ferroelectric properties and ion conductivity (including proton conductivity), in traditional clay mineral-kaolinite, as revealed by our results, offer unique possibilities compared to conventional applications. These findings illuminate the design and preparation of technologically important multi-functional materials based on the traditional layered clay mineral, potentially rejuvenating its use in various fields.

Additionally, the unknown real alignments of guest molecules in the interlayer space pose remaining challenges since experimental crystal structures for these intercalated hybrids have not been obtained. So, seeking the powerful method to classify the actual situation of basal space of intercalated kaolinites and the origin of the multiple properties is strongly needed. Actually, theoretical simulations such as DFT calculations and/or molecular dynamics (MD) as well as the high-throughput calculations and AI-assisted methodology (such as machine learning , deep-learning potential, etc.) can be utilized as a suitable and powerful approach [87, 88].

In the pursuit of this research direction, an additional promising avenue for intercalated kaolinites involves the exploration of new intercalated agents that can displace existing ones. This exploration aims to establish a correlation between the structural characteristics and the diverse functional properties, expanding beyond the investigation of the rich and technologically important physical properties exhibited by these intercalated kaolinite compounds. These efforts should be done by relying on a more abundant experimental database and will be studied further in future.

ACKNOWLEDGMENTS

The authors thank the financial supports by the National Natural Science Foundation of China (Grant no. 21671100 and 22103054). H.Y. is supported by grants from startup supports of Soochow University. H.Y. thanks China Postdoctoral Science Foundation (2019M660128) and Jiangsu Planned Projects for Postdoctoral Research Funds (2021K184B) for financial support. This work was partly supported by Collaborative Innovation Center of Suzhou Nano Science & Technology, the Priority Academic Program Development of the Jiangsu Higher Education Institutions, the 111 Project, Joint International Research Laboratory of Carbon-Based Functional Materials and Devices.

REFERENCES

[1] M. I. Carretero and G. Lagaly, Appl. Clay Sci., 2007, 36, 1. https://doi.org/10.1016/j.clay.2006.05.010

[2] R. T. Martin, S. W. Bailey, D. D. Eberl, D. S. Fanning, S. Guggenheim, H. Kodama, D. R. Pevear, J. Srodon and F. J. Wicks, Clays Clay Miner., 1991, 39, 333.

[3] H. H. Murray, Appl. Clay Sci., 2000, 17, 207. https://doi.org/10.1016/S0169-1317(00)00016-8

[4] Z. Ding, J. T. Kloprogge, R. L. Frost, G. Q. Lu and H. Y. Zhu, J. Porous Mater., 2001, 8, 273. https://doi.org/10.1023/A:101311303091

[5] X. Y, Zhu, C. J. Yan and J. Y. Chen, Appl. Clay Sci., 2012, 55, 114. https://doi.org/10.1016/j.clay.2011.11.001

[6] F. Bergaya and G. Lagaly, in General Introduction: Clays, Clay Minerals, and Clay Science, Handbook of Clay Science: Developments in Clay Science, ed., F. Bergaya, B. K. G. Theng, G. Lagaly, Elsevier, Amsterdam, 2006. vol. 1, p. 1. https://doi.org/10.1016/S1572-4352(05)01001-9

[7] W. N. Martens, R. L. Frost, J. Kristóf and E. Horvath, J. Phys. Chem. B, 2002, 106, 4162. https://doi.org/10.1021/jp0130113

[8] F. Franco, L. A. Pérez-Maqueda and J. L. Pérez-Rodríguez, J. Colloid Interface Sci., 2004, 274, 107. https://doi.org/10.1016/j.jcis.2003.12.003

[9] S. Letaief and C. Detellier, J. Mater. Chem., 2005, 15, 4734.S.-P. Zhao, Y. Guo, M.-M. Zhu, J. Wang, X.-L. Feng, Q. Qiao and H. Xu, Clays Clay Minerals, 2019, 67, 461. https://doi.org/10.1007/s42860-019-00036-x

[10] R. L. Frost, O. B. Locos, J. Kristóf and J. T. Kloprogge, Vib. Spectrosc., 2001, 26, 33. https://doi.org/10.1016/S0924-2031(01)00108-4

[11] K. Wada, Am. Mineral., 1959, 44, 153. https://doi.org/10.1093/genetics/44.2.153

[12] K. Wada, Am. Mineral., 1961, 46, 78. https://doi.org/10.4144/rpsj1954.1961.1

[13] R. L. Frost, J. Kristóf, L. Rintoul, J. T. Kloprogge, Spectrochim. Acta A: Mol. Biomol. Spectrosc., 2000, 56, 1681. https://doi.org/10.1016/S1386-1425(00)00223-7

[14] H. Ming, Clay Miner., 2004, 39, 349. https://doi.org/10.1180/0009855043930140

[15] S. Letaief and C. Detellier, J. Therm. Anal. Calorim., 2011, 104, 831. https://doi.org/10.1007/s10973-010-1269-8

[16] J. E. F. C. Gardolinski and G. Lagaly, Clay. Miner., 2005, 40, 537. https://doi.org/10.1180/0009855054040190

[17] D. Zhang, C. H. Zhou, C. X. Lin, D. S. Tong and W. H. Yu, Appl. Clay Sci., 2010, 50, 1. https://doi.org/10.1016/j.clay.2010.06.019

[18] E. Horváth, J. Kristóf, R. L. Frost, Appl. Spectrosc. Rev., 2010, 45, 130. https://doi.org/10.1080/05704920903435862

[19] H. F. Cheng, Q. F. Liu, J. Yang, S. J. Ma and R. L. Frost, Thermochim. Acta, 2012, 545, 1. https://doi.org/10.1016/j.tca.2012.04.005

[20] N. Bizaia, E. H. de Faria, G. P. Ricci, P. S. Calefi, J. Nassar Eduardo, K. A. D. F. Castro, S. Nakagaki, K. J. Ciuffi, R. Trujillano, M. A. Vicente, A. Gil and S. A. Korili, ACS Appl. Mater. Interfaces, 2009, 1, 2667. https://doi.org/10.1021/am900556b

[21] K. R. Kumrić, A. B. Đukić, T. M. Trtić-Petrović, N. S. Vukelić, Z. Stojanović, J. D. G. Novaković and L. L. Matović, Ind. Eng. Chem. Res., 2013, 52, 7930.

[22] E. H. de Faria, E. J. Nassar, K. J. Ciuffi, M. A. Vicente, R. Trujillano, V. Rives and P. S. Calefi, ACS Appl. Mater. Interfaces, 2011, 3, 1311. https://doi.org/10.1021/am2001086

[23] R. Takenawa, Y. Komori, S. Hayashi, J. Kawamata and K. Kuroda, Chem. Mater., 2001, 13, 3741. https://doi.org/10.1021/cm010095j

[24] Y. Suzuki, Y. Tenma, Y. Nishioka, J. Kawamata, Chem. Asian J., 2012, 7, 1170. https://doi.org/10.1002/asia.201200049

[25] S. P. Zhao, H. Gao, X. M. Ren, G. J. Yuan and Y. N. Lu, J. Mater. Chem., 2012, 22, 447. https://doi.org/10.1039/C1JM13115J

[26] X. P. Li, H. Yang, Z. F. Tian, J. L. Liu and X. M. Ren, Dalton Trans., 2014, 44, 4665. https://doi.org/10.1039/C4DT04018J

[27] (a) Q. Qiao, H. Yang, J. L. Liu, S. P. Zhao and X. M. Ren, Dalton Trans., 2014, 14, 5427; (b) Q. Qiao, Y. N. Ding, S. P. Zhao, L. Li, J. L. Liu and X. M. Ren, Inorg. Chem. Front., 2017, 4, 1405. https://doi.org/10.1039/c3dt52930d https://doi.org/10.1039/C7QI00341B

[28] G. Z. Zou, H. Gao, J. L. Liu, S. P. Zhao, Z. F. Tian and X. M. Ren, RSC Adv., 2013, 3, 23596. https://doi.org/10.1039/c3ra40579f

[29] L. T. Ren, X. P. Li, J. L. Liu and X. M. Ren, J. Solid State Chem., 2015, 232, 31. https://doi.org/10.1016/j.jssc.2015.09.001

[30] X. Q. Huang, H. Yang, S. P. Zhao, J. L. Liu and X. M. Ren, Eur. J. Inorg. Chem., 2015, 4708. https://doi.org/10.1002/ejic.201500550

[31] (a) H. Yang, X. Sun, S. X. Liu, J. L. Liu and X. M. Ren, ChemistrySelect, 2016, 1, 2181; (b) H. Yang, X. Sun, S. X. Liu, Y. Zou, L. Li, J. L. Liu and X. M. Ren, New J. Chem., 2016, 40, 10233. https://doi.org/10.1002/slct.201600217 https://doi.org/10.1039/C6NJ02386J

[32] S. X. Liu, C. Xue, H. Yang, X. Q. Huang, Y. Zou, Y. N. Ding, L. Li and X. M. Ren, Solid State Sci., 2017, 74, 95. https://doi.org/10.1016/j.solidstatesciences.2017.10.007

[33] D. L. Bish, Clays Clay Miner., 1993, 41, 738. https://doi.org/10.1346/CCMN.1993.0410613

[34] H. H. Murray, in Kaolins in Kaolin Genesis and Utilization, ed., W. Bundy and C. Harvey, Clay Miner. Soc., Boulder, CO, 1993. https://doi.org/10.1346/CMS-SP-1

[35] P. M. Costanzo and J. R. F. Giese, Clays Clay Miner., 1985, 33, 415. https://doi.org/10.1346/CCMN.1985.0330507

[36] J. G. Thompson and C. Cuff, Clays Clay Miner., 1985, 33, 490. https://doi.org/10.1346/CCMN.1985.0330603

[37] P. J. R. Uwins, I. D. R. Mackinnon, J. G. Thompson and A. J. E. Yago, Clays Clay Miner., 1993, 41, 707. https://doi.org/10.1346/CCMN.1993.0410609

[38] J. J. Tunney and C. Detellier, Chem. Mater., 1996, 8, 927. https://doi.org/10.1021/cm9505299

[39] T. A. Elbokl and C. Detellier, J. Phys. Chem. Solids, 2006, 67, 950. https://doi.org/10.1016/j.jpcs.2006.01.008

[40] R. L. Frost, J. Kristóf, E. Mako and J. T. Kloprogge, Langmuir, 2000, 16, 7421. https://doi.org/10.1021/la9915318

[41] E. P. Giannalis, Adv. Mater., 1996, 81, 29. https://doi.org/10.1002/adma.19960080104

[42] (a) A. Weiss, Angew. Chem. Int. Ed., 1963, 2, 697; (b) A. Weiss, W. Thielepape and H. Orth, Proc. Int.Clay Conf., 1966, 1, 277. https://doi.org/10.1002/anie.196306971

[43] R. L. Frost, J. Kristóf, G. N. Paroz, J. T. Kloprogge, J. Colloid Interface Sci., 1999, 208, 216. https://doi.org/10.1006/jcis.1998.5780

[44] (a) R. L. Frost, J. Kristóf, E. Horváth and J. T. Kloprogge, J. Colloid Interface Sci., 1999, 214, 380; (b) R. L. Frost, J. Kristóf, E. Horváth and J. T. Kloprogge, Langmuir, 1999, 15, 8787. https://doi.org/10.1006/jcis.1999.6209 https://doi.org/10.1021/la981755a

[45] R. L. Frost, J. Kristóf, E. Horváth, W. N. Martens and J. T. Kloprogge, J. Colloid Interface Sci., 2002, 251, 350. https://doi.org/10.1006/jcis.2002.8384

[46] (a) T. Itagaki, Y. Komori, Y. Sugaharaa and K. Kuroda, J. Mater. Chem., 2001, 11, 3291; (b) W. N. Martens, R. L. Frost, J. Kristóf, E. Horváth, J. Phys. Chem. B, 2002, 106, 4162; (c) M. Janek, K. Emmerich, S. Heissler and R. Nüesch, Chem. Mater., 2007, 19, 684; (d) J. Matusik, E. Scholtzová and D. Tunega, Clays Clay Miner., 2012, 60, 227. https://doi.org/10.1039/b100746g https://doi.org/10.1021/jp0130113 https://doi.org/10.1021/cm061481+ https://doi.org/10.1346/CCMN.2012.0600301

[47] R. L. Frost, J. Kristóf, E. Horváth and J. T. Kloprogge, J. Colloid Interface Sci., 2001, 239, 126. https://doi.org/10.1006/jcis.2001.7542

[48] R. L. Frost, J. Kristóf, E. Horváth, W. N. Martens and J. T. Kloprogge, J. Colloid Interface Sci., 2002, 246, 164. https://doi.org/10.1006/jcis.2001.8011

[49] R. L. Frost, J. Kristóf, G. N. Paroz, T. H. Tran and J. T. Kloprogge, J. Colloid Interface Sci., 1998, 204, 227. https://doi.org/10.1006/jcis.1998.5604

[50] S. L. Olejnik, J. Phys. Chem., 1968, 72, 241. https://doi.org/10.1021/j100847a045

[51] G. K. Dedzo, S. Letaief and C. Detellier, J. Mater. Chem., 2012, 22, 20593. https://doi.org/10.1039/c2jm34772e

[52] T. J. James and D. Christian, Clays Clay Miner., 1994, 42, 552. https://doi.org/10.1346/CCMN.1994.0420506

[53] H. F. Emerson, J. L. Omar, J. C. Katia, J. N. Eduardo, A. V. Miguel, T. Raquel and S. C. Paulo, J. Colloid Interface Sci., 2009, 335, 210.

[54] P. Sidheswaran, A. N. Bhat and P. Ganguli, Clays Clay Miner., 1990, 38, 29. https://doi.org/10.1346/CCMN.1990.0380104

[55] K. B. Brandt, T. A. Elbokl and C. Detellier, J. Mater. Chem., 2003, 13, 2566. https://doi.org/10.1039/b306468a

[56] E. Makó, J. Kristóf, E. Horvath and V. Vagvolyi, J. Colloid Interface Sci., 2009, 330, 367. https://doi.org/10.1016/j.jcis.2008.10.054

[57] G. Rutkai, E. Makó and T. Kristóf, J. Colloid Interface Sci., 2009, 334, 65. https://doi.org/10.1016/j.jcis.2009.03.022

[58] R. K. Vempati, M. Y. A. Mollah, G. R. Reddy, D. L. Cocke and H. V. Lauer Jr, J. Mater. Sci., 1996, 31, 1255. https://doi.org/10.1007/BF00353104

[59] J. M. Adams and G. Waltl, Clays Clay Miner., 1980, 28, 130. https://doi.org/10.1346/CCMN.1980.0280209

[60] É. Makó, J. Kristóf, E. Horváth, V. Vágvölgyi, J. Colloid Interface Sci., 2009, 330, 367. https://doi.org/10.1016/j.jcis.2008.10.054

[61] B. Caglar, J. Mol. Struct., 2012, 1020, 48. https://doi.org/10.1016/j.molstruc.2012.03.061

[62] R. L. Frost, J. Kristóf, G. N. Paroz, J. T. Kloprogge, Phys. Chem. Miner., 1999, 26, 257. https://doi.org/10.1007/s002690050185

[63] K. Tsunematsu and H. Tateyama, J. Am. Ceram. Soc., 1999, 82, 1589. https://doi.org/10.1111/j.1151-2916.1999.tb01963.x

[64] E. W. Hope and J. A. Kittrick, Am. Mineral., 1964, 49, 859.

[65] J. E. F. C. Gardolinski and G. Lagaly, Clay Miner., 2005, 40, 537. https://doi.org/10.1180/0009855054040190

[66] Y. Kuroda, K. Ito, K. Itabashi and K. Kuroda, Langmuir, 2011, 27, 2028. https://doi.org/10.1021/la1047134

[67] S. Letaief and C. Detellier, Langmuir, 2009, 25, 10975. https://doi.org/10.1021/la901196f

[68] M. D. R. Cruz and F. I. F. Duro, Clay Miner., 1999, 34, 565. https://doi.org/10.1180/000985599546451

[69] R. L. Ledoux and J. L. White, Science, 1964, 143, 244. https://doi.org/10.1126/science.143.3603.244

[70] N. E. Hill, V. E. Vaughan, A. H. Price and M. Davies, in Dielectric properties and molecular behavior, The van Norstrand Series in Physical Chemistry, ed. T. M. Sugden, New York, Toronto, Melbourne, 1969, p. 282.

[71] K. Orzechowski, T. Słonka and J. Głowinski, J. Phys. Chem. Solids, 2006, 67, 915. https://doi.org/10.1016/j.jpcs.2006.03.001

[72] K. Leluk, K. Orzechowski, K. Jerie, A. Baranowski, T. Slonka and J. Glowinski, J. Phys. Chem. Solids, 2010, 71, 827. https://doi.org/10.1016/j.jpcs.2010.02.008

[73] K. S. Cole and R. H. Cole, J. Chem. Phys., 1941, 9, 341. https://doi.org/10.1063/1.1750906

[74] V. K. Syal, S. Chauhan and U. Kumari, Indian J. Pure Appl. Phys., 2005, 43, 844.

[75] S. Cabani, P. Gianni, V. Mollica and L. Lepori, J. Solution Chem., 1981, 10, 563. https://doi.org/10.1007/BF00646936

[76] G. J. Goldsmith and J. G. White, J. Chem. Phys., 1959, 31, 1175. https://doi.org/10.1063/1.1730568

[77] S. Letaief, T. Diaco, W. Pell, S. I.. Gorelsky and C. Detellier, Chem. Mater., 2008, 20, 7136. https://doi.org/10.1021/cm800758c

[78] J. Halbritter, Phys. Rev. B: Condens. Matter, 1993, 48, 9735. https://doi.org/10.1103/PhysRevB.48.9735

[79] K. D. Kreuer, S. J. Paddison, E. Spohr and M. Schuster, Chem. Rev., 2004, 104, 4637. https://doi.org/10.1021/cr020715f

[80] H. B. Luo, L. T. Ren, W. H. Ning, S. X. Liu, J. L Liu and X. M. Ren, Adv. Mater., 2016, 28, 1663. https://doi.org/10.1002/adma.201504591

[81] (a) M. Sadakiyo, T. Yamada, K. Honda, H. Matsui and H. Kitagawa, J. Am. Chem. Soc., 2014, 136, 7701; (b) S. S. Bao, K. Otsubo, J. M. Taylor, Z. Jiang, L. M. Zheng and H. Kitagawa, J. Am. Chem. Soc., 2014, 136, 9292. https://doi.org/10.1021/ja5022014 https://doi.org/10.1021/ja505916c

[82] T. Kundu, S. C. Sahoo, R. Banerjee, Chem. Commun., 2012, 48, 4998. https://doi.org/10.1039/c2cc31135f

[83] J. M. Taylor, K. W. Dawson and G. K. H. Shimizu, J. Am. Chem. Soc., 2013, 135, 1193. https://doi.org/10.1021/ja310435e

[84] H. P. Ma, B. L. Liu, B. Li, L. M. Zhang, Y. G. Li, H. Q. Tan, H. Y. Zang and G. S. Zhu, J. Am. Chem. Soc., 2016, 138, 5897. https://doi.org/10.1021/jacs.5b13490

[85] C. A. Oliveira Ribeiro, Y. Vollaire, A. Sanchez-Chardi, H. Roche, France. Aquat. Toxicol., 2005, 74, 53. https://doi.org/10.1016/j.aquatox.2005.04.008

[86] S. S. Gupta, K. G. Bhattacharyya, J. Hazard. Mater., 2006, 128, 247. https://doi.org/10.1016/j.jhazmat.2005.08.008

[87] T. Ohkubo, A. Takei, Y. Tachi, Y. Fukatsu, K. Deguchi, S. Ohki and T. Shimizu, J. Phys. Chem. A, 2023, 127, 973. https://doi.org/10.1021/acs.jpca.2c08880

[88] K. Kobayashi, A. Yamaguchi, M. Okumura, Appl. Clay Sci. 2022, 228, 106596. https://doi.org/10.1016/j.clay.2022.106596

Received on 15-05-2023 Accepted on 19-06-2023 Published on 24-06-2023

DOI: https://doi.org/10.31875/2410-4701.2023.10.07